



Cite this: *RSC Adv.*, 2026, **16**, 2449

## A novel method for pH mediated electroflocculation in saltwater systems

Galen Dennis, \* Devin A. J. Karns and Matthew C. Posewitz

Microalgae represent an untapped resource for novel biomass production and the subsequent production of feed, food and fuels. Harvesting micro-algal cultures is a technical challenge due to the relatively low concentration of biomass of even dense algal cultures. Flocculating the cells in culture before these steps can simplify harvesting by increasing filterability and settling velocity. Electroflocculation has the advantages of technical simplicity, and potential for integration into a continuous treatment process. In seawater, it is possible to flocculate cells using a non-sacrificial anode such as graphite or titanium, however, this method is complicated by the production of  $\text{Cl}_2$  gas and oxidative chloride compounds at the anode. The diffusion of these products into solution causes damage to cells. This study shows that cells can be protected from these oxidative products and flocculated by integrating a regenerated cellulose membrane into the electrolysis system between the culture and anode solution. The viability of this technique is demonstrated by flocculation tests on the productive saltwater microalga *Picochlorum celeri* TG2, which is difficult to harvest due to slow settling and small cell sizes. By using non-sacrificial electrodes with membrane protection, the settling efficiency of the strain was increased, with an  $\sim 95\%$  clarification and a compaction factor below 0.2 (after treatment and settling for one hour). The added power requirements across a range of current densities and biomass concentrations are also reported. The best volumetric energy consumption tested was at 0.86 A/L requiring an average of  $3.1 \text{ kWh m}^{-3}$  ( $\pm 0.1 \text{ kWh m}^{-3}$ ). Settling efficiency and energy requirement on a biomass basis was found to be independent of biomass in the  $0.5\text{--}1.6 \text{ g L}^{-1}$  range tested, with the lowest biomass energy requirement achieved at  $3.0 \text{ kWh kg}$  ( $\pm 0.2 \text{ kWh kg}$ ).

Received 10th October 2025  
 Accepted 25th December 2025

DOI: 10.1039/d5ra07757e  
[rsc.li/rsc-advances](http://rsc.li/rsc-advances)

## 1. Introduction

### 1.1 Flocculation as a pretreatment step before harvesting microalgae

Microalgae are single-celled photosynthetic organisms composing an underutilized source of biomass that can be produced in non-arable and saline environments. Some strains produce unique metabolites such as poly-unsaturated fatty acids and pigments which have demonstrated useful antioxidant and/or photoprotective properties.<sup>1</sup> The marine alga *Picochlorum celeri* TG2 is a strain capable of achieving exceptional productivity ( $\sim 40 \text{ gm}^{-2}\text{day}$ ) in outdoor raceway ponds.<sup>2-4</sup> A critical aspect of this cultivation is that it is photoautotrophic and is grown in seawater as a sustainable method of biomass production. Current bottlenecks to industrial microalgal cultivation include the energy efficiency of photosynthesis,<sup>5</sup> the intrinsic biomass value,<sup>6</sup> and biomass harvesting and processing.<sup>4</sup>

Harvesting photoautotrophically grown microalgal cultures is complicated by several factors. First the small cell size and single-celled nature of these organisms mean that the cells can stay uniformly distributed through the liquid medium, and settling

takes a relatively long time depending on the respective densities of the cells and medium.<sup>7</sup> Second, even those cultures that achieve high biomass concentrations ( $1\text{--}10 \text{ g L}^{-1}$ ) are still 99.9–99.0%  $\text{H}_2\text{O}$ , and only 0.1–1.0% dry mass. Before this biomass can be processed, it must be dewatered as a means of reducing cost and simplifying downstream extraction and/or refinement.<sup>8</sup>

There are a variety of options available for dewatering (harvesting) microalgae, including dead end or cross flow filtration, centrifugation, and flocculation with flotation/settling.<sup>9</sup> Flocculation is an effective method for concentrating cells before these harvesting approaches. One approach utilizes electric current to induce cell-cell adhesion by overcoming the repulsion of negatively charged cell walls.<sup>10</sup> The energy requirement to harvest cells through filtration and/or time required for settling can be reduced by flocculating the cells into larger clusters. Moreover, this improvement is potent, as both properties are proportional to the second power of the particle radius. While flocculation refers generally to aggregation of suspended cell by chemical, pH-mediated, or biological means, electroflocculation specifically uses electrical current to induce the aggregation.

Electrically induced flocculation is also referred to as electrocoagulation-flootation (ECF).<sup>11</sup> This term encompasses the use of both sacrificial and inert electrodes. There are a variety of mechanisms that may occur depending on the electrode

Department of Chemistry, Colorado School of Mines, 1500 Illinois Street, Golden, CO, 80401, U.S.A. E-mail: [gdennis@mines.edu](mailto:gdennis@mines.edu)



material and electrolyte composition of the liquid. One commonly explored method is the use of a sacrificial metal anode (typically a relatively inexpensive metal such as iron or aluminum) that dissolves during electrolysis, dispersing cations into the culture which act as bridges to overcome negatively charged cell-cell repulsion. This method works in fresh and saline water, and is efficient in terms of speed, simplicity, and energy return on investment. However it has two major drawbacks: the contamination of biomass with metal ions, and the steady degradation of the anode over time.<sup>12</sup>

By comparison, inert (non-sacrificial) electrodes bypass the issues presented by sacrificial electrodes by using a stable electrode material (usually titanium oxide or graphite) while still inducing flocculation. In the freshwater case, this is proposed to occur by migration of cells along the ion gradient until the negative cell charge is neutralized by cations near the cathode.<sup>9,13</sup> In the saltwater case, flocculation is also induced by the formation of magnesium hydroxide ( $Mg(OH)_2$ ) and calcium carbonate ( $CaCO_3$ ).<sup>14</sup> Magnesium hydroxide precipitate retains a partial positive electronegative character that bridges negatively charged cell walls, and the precipitation of calcium salts entraps cells as it settles or floats in the culture.<sup>15</sup> This method is used for both clarification in wastewater treatment, and is referred to as sweep coagulation.<sup>16</sup> The relatively high concentration of ions (~4%) in seawater leads to reduced resistance and improved energy efficiency compared to freshwater.<sup>17</sup>

As in freshwater, current is generated through  $H_2O$  splitting.<sup>18</sup> In addition, when running current through  $H_2O$  containing NaCl with non-sacrificial electrodes  $Cl_2$  gas is produced at the anode. Hydrogen gas is produced at the cathode and forms bubbles which carry cells to the top of the culture (flootation). If the floated biomass is mixed and the  $H_2$  is allowed to outgas, the flocculated cells will also settle. In addition to  $H_2$ ,  $OH^-$  is produced and raises the pH around the cathode. Magnesium and calcium salt formation and precipitation occur by a seawater pH increase. This process is reversible by titrating harvested cultures to a lower pH with acid.<sup>14</sup>

## 1.2 Microalgal electroflocculation with non-sacrificial electrodes

A major issue with non-sacrificial electrode flocculation is the toxic effects of chlorine and  $ClO_x$  ion production in the microalgal culture. Because of this problem, there is minimal literature on using inert electrodes for electroflocculation in seawater. One publication described electrode solution separation using a technique called salt bridge electroflocculation.<sup>19</sup> This approach relies on a porous ceramic container filled with a saline agar mix to separate the anode and cathode and the use of non-sacrificial carbon electrodes. *Nannochloropsis oculata* was grown to  $1.4\text{ g L}^{-1}$  and tested in  $350\text{ mL}$  batches using this technique, reporting a best energy consumption of  $1.5\text{ kWh kg}^{-1}$  with a recovery efficiency of 90.4%, measured on an OD basis after treating for 45 min at  $300\text{ mA}$ .<sup>19</sup>

In contrast, another study explored non-sacrificial electrode flocculation of *Dunaliella salina* without anode–cathode separation. The generation of  $Cl_2$  was mentioned, but its culture

toxicity was not addressed. Despite this, under optimized conditions only 20% of cells were estimated to remain intact after flocculation. The algal cultures were tested in  $500\text{ mL}$  batches grown in hypersaline  $120\text{ g L}^{-1}$  NaCl artificial saltwater medium. A current of  $0.7\text{ A}$  for 6 min showed the best harvesting efficiency with a power consumption of  $0.63\text{ kWh m}^{-3}$ .<sup>20</sup> The results of this study show that protection is needed for cells being electroflocculated in saline systems. Other non-sacrificial electrode studies focus only on freshwater algae when using inert electrodes, and these studies require no protection against chloride oxidation products. As the mechanism for flocculation is fundamentally different for freshwater cultures, a comparison between freshwater and saltwater non-sacrificial ECF is difficult.

Guldhe *et al.* published work on non-sacrificial electrode flocculation of the freshwater algae *Ankistrodesmus falcatus* and *Scenedesmus obliquus* in BG-11 medium using carbon electrodes.<sup>21</sup> Tests were conducted on  $1\text{ L}$  cultures at  $2.88\text{ g L}^{-1}$  for *A. falcatus* and  $2.76\text{ g L}^{-1}$  for *S. obliquus*. An optimum treatment time was reported to be 30 min at  $1\text{ A}$  leading to a total power consumption of  $1.76\text{ kWh kg}^{-1}$  and ~90% recovery efficiency. In a similar study, Misra *et al.* cultivated and tested non-sacrificial electrode harvesting of  $2.4\text{ g L}^{-1}$  cultures of *Scenedesmus obliquus*. A maximum recovery of 83% at  $1.5\text{ A}$ , with  $6\text{ g L}^{-1}$  NaCl in BG-11 medium was found, with a power consumption of  $3.84\text{ kWh kg}^{-1}$ .<sup>15</sup> Finally, Li *et al.* harvested *Chlorella vulgaris* by using a stainless steel cathode and a platinum-plated titanium alloy anode.<sup>22</sup> A 90% harvesting efficiency was reported with  $30\text{ kWh kg}^{-1}$  energy consumption at  $3\text{ A}$  current for 50 min. In summary, freshwater electroflocculation with inert electrodes has generally been reported to achieve a harvesting efficiency of >90% under the best conditions found and the best requirement reported was  $1.76\text{ kWh kg}^{-1}$ . These values, and the energy requirements found by Hou *et al.* represent benchmark values for other electroflocculation studies to improve upon.<sup>19</sup>

To make non-sacrificial electrode flocculation viable in seawater, scalable methods must be developed that protect the algal culture from oxidative species produced at the anode during electrolysis. This study describes a novel approach for protecting microalgae from oxidative species formation during electroflocculation with inert electrodes using a dialysis membrane is sufficient to protect algal cells in the cathode compartment from oxidative products of the anode. *Picochlorum celeri* TG2 is used as a model strain as it has shown impressive growth in saline media over the past decade,<sup>3,4</sup> and has also emerged as a promising chassis for genetic engineering.<sup>23,24</sup> However, for *P. celeri* TG2, challenges with harvesting are exacerbated by the small cell size ( $2\text{--}3\text{ }\mu\text{m}$ ) increasing settling time and/or requiring smaller pore filters to fully separate algal cells from the media. Small increases in the effective size of *P. celeri* TG2 would have potent impacts on the harvestability of this strain. A previous study has explored flocculation in the closely related strain *Picochlorum oklahomensis* using a variety of approaches including biopolymer, pH, and sacrificial anode electroflocculation.<sup>25</sup> However, there is no work with non-sacrificial electrodes, and this study provides complementary data. In addition, despite its excellent outdoor



productivities, the intrinsic biomass value of *P. celeri* is low compared to other candidate strains for outdoor growth.<sup>6</sup> In combination, these traits make *P. celeri* TG2 a relevant strain for testing new approaches for flocculation.

## 2. Materials and methods

### 2.1 Biomass cultivation and measurements

Algal cultures were grown in Marine Dense medium formulated as previously described.<sup>2,26</sup> Cultivation was done under 1% CO<sub>2</sub> and 500  $\mu$ mol photosynthetically active radiation (PAR) at 33 °C constant temperature. Cultures were grown to an optical density at 750 nm > 3.0 and then diluted to the approximate desired biomass density based on initial ash-free dry weight (AFDW) measurements as indicated. Prior to dilution, cultures were kept at 4 °C in the dark to minimize biomass loss. During electrolysis, 10 mL culture samples were taken at 0, 5, 20, 30, 40, and 60 min from the culture for analysis. For each sample, the order of measurements was as follows: (1) Samples were mixed and an optical density measurement taken, (2) a second optical density measurement was taken after an hour of settling, (3) pH values were recorded for each sample, (4) the samples were re-suspended and mass measurements were taken at the 0.7  $\mu$ m and 10  $\mu$ m pore size level. In addition to this, 1 mL samples were taken from the anode solution for pH measurements at each timepoint, and 100 mL of volume was taken at the final timepoint (60 min) for pH and cell count measurements before and after neutralization.

Optical density measurements were taken at 750 nm using a P4 UV-visible spectrophotometer (VWR, U.S.A.). Samples were diluted to an optical density <1.0 before recording measurements. Cell counts were performed on the same samples using an Attune NxT flow cytometer (Life Technologies, U.S.A.). Counts were gated based on chlorophyll autofluorescence.

Dry weight and AFDW measurements at 0.7  $\mu$ m pore size were measured using fiberglass filters (Part number – 66258, Pall Corporation, U.S.A.). Filters were pre-treated by washing with 10 mL of 0.5 M ammonium bicarbonate and pre-ashing at 550 °C for

20 min. Samples were filtered under vacuum and washed with 3 sample volume equivalents of 0.5 M ammonium formate. AFDW samples were ashed for at least 2 h at 550 °C and measured for ash weight after cooling to room temperature. Dry weights at 10  $\mu$ m pore size were measured using the same technique with polycarbonate membrane filters (Part number – TCTPO4700, Sigma-Aldrich, U.S.A.). AFDW could not be measured with polycarbonate filters as they are combustible at 550 °C. All filtered samples were dried overnight at 105 °C then measured for dry weight.

### 2.2 pH measurement

Samples were allowed to equilibrate with air before initial (pre-treatment) pH measurements. For seawater only samples the liquid was stirred at room temperature for at least 1 h prior to measurement, whereas algal cultures were bubbled with air for at least 30 min to overcome any effects from respiration or photosynthetic activity. A pH probe (UltraBASIC, Denver Instrument, U.S.A.) was calibrated using standards for pH 4, 7 and 10 (Part numbers – BDH5018, BDH0194, and BDH5072, respectively, VWR Chemicals, U.S.A.). Samples of at least 1 mL collected in 10 mL glass test tubes were measured while continuously mixed by vigorous swirling.

### 2.3 Benchtop scale flocculation tests

Fig. 1 shows the general experimental configuration used for this study and Fig. 2 provides a detailed representation of the treatment system, including dimension and volumes. Culture (cathode) volume was kept at 500 mL, and the anode solution volume at 100 mL. At these volumes, the submerged surface area of the cathode was 65 cm<sup>2</sup>, while the submerged surface area of the anode was 98 cm<sup>2</sup>. The submerged membrane surface area for the cathode and anode solutions were 30 cm<sup>2</sup> and 48 cm<sup>2</sup> respectively. A vacuum snorkel was kept above the solution to safely remove gasses generated during the test.

Electrodes were kept 12 cm apart, and the anode was centered in the anode chamber with a 0.5 cm distance from the membrane for the graphite electrode. At each time point, 1 mL

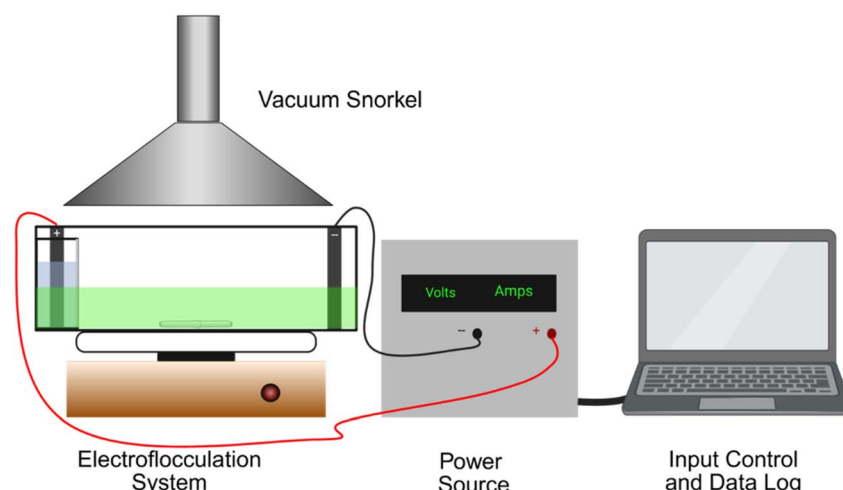


Fig. 1 Illustration of benchtop system used, with current provided through 1 × 10 × 10 cm graphite electrodes from a power supply controlled and logged by computer.



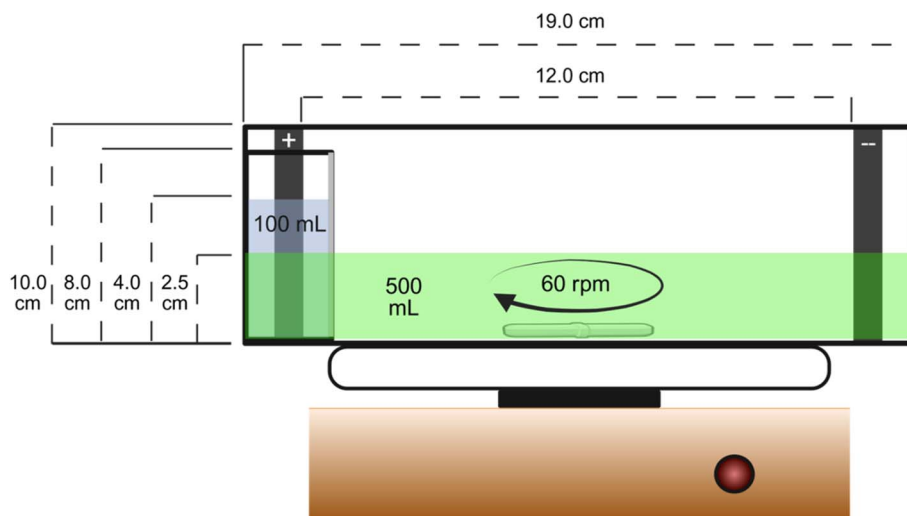


Fig. 2 A detailed sketch of the electrolysis system including volumes used. Note that the electrodes length is 10 cm. Sketch is not to scale with dimensions adjusted for ease of viewing.

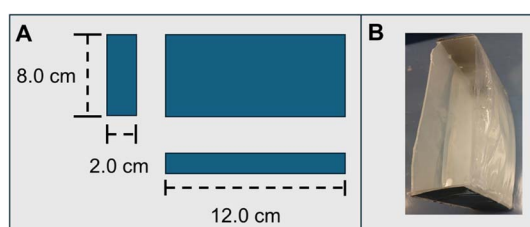


Fig. 3 (A) Dimensions of the anode chamber are used to isolate the electrode solutions with a membrane. (B) Photograph of the physical chamber filled with 100 mL seawater.

was removed from the anode solution and 10 mL removed from the cathode solution with the difference in volume being accounted for in all calculations with a volume dependence. These samples were used for pH and biomass measurements as described in section 3.1 and 3.2. Current, voltage, and treatment time were recorded at 3 s intervals by a BK Precision® power source (Product number – 1687B, B&K Precision Corporation, U.S.A.) using the manufacturer's software. If a buildup of flocculated cells was observed behind the cathode or anode chamber, then the electrode and chamber were moved forward and back by one or two centimeters before sampling to allow the culture to homogenize. Electrodes were rinsed with DI water between tests, and the cathode was wiped down with a paper towel to remove excess cell and salt buildup at the culture surface height. To verify previous study results<sup>20</sup> electrodes were periodically dried overnight at 105 °C and weighed to ensure that mass was not lost (data not shown).

Anode chambers were made by folding a regenerated cellulose membrane (12–14 kDa molecular weight cutoff, Part number – 1385200, School Specialty, U.S.A.) over the polycarbonate casing (Fig. 3). The membrane was taped into place, and the inner membrane seam and the outer tape seams sealed by a layer of plastic adhesive (Part number – PR40, HongKong Guoelephant Group, U.S.A.). The adhesive was allowed to dry for a minimum of 2 h before testing. Membranes were reused between tests unless a tear developed, in which case it was replaced. Between tests the anode chamber was cleaned with deionized H<sub>2</sub>O and gently dried with a paper towel, after which it was kept submerged in deionized H<sub>2</sub>O to prevent dehydration of the membrane.

Calculations for the compaction factor, settling efficiency, volumetric flocculation cost, and biomass flocculation cost were done as shown in eqn (1)–(4), respectively. Measurements for settling efficiency and compaction factor were both taken one hour after settling. The clarified supernatant was sampled at the top of the test tube used for settling.

$$\text{Compaction factor} = \frac{\text{settled biomass height}}{\text{total sample height}} \quad (1)$$

$$\text{Settling efficiency} = \frac{\text{settled sample supernatant OD}_{750}}{\text{mixed sample OD}_{750}} \times 100 \quad (2)$$

$$\text{Volumetric treatment cost} = \frac{\text{electricity use (kWh)}}{\text{culture volume (L)}} \quad (3)$$

$$\text{Biomass flocculation cost} = \frac{\text{electricity use (kWh)}}{\text{AFDW (g L}^{-1}\text{)} \times \frac{1 \text{ kg}}{1000 \text{ g}} \times \frac{\text{settling efficiency}}{100} \times \text{volume (L)}} \quad (4)$$



### 3. Results and discussion

#### 3.1 Electricity requirement at various current setpoints

A series of tests across three current setpoints were conducted to assess the effect of current on algal flocculation. The data points represented in Fig. 4–7 are the average of three independent tests with a single replicate for each current setpoint being collected during each test. For these tests, the average AFDW and standard deviations were  $0.29 (\pm 0.02)$ ,  $0.38 (\pm 0.02)$ , and  $0.68 (\pm 0.06)$  g L<sup>-1</sup>. Average current and voltages across 40 min of treatment for the setpoints of 1 A/L, 2 A/L, and 4 A/L are shown in Fig. 4. The average (+/- standard deviation) voltages across the treatment time course at these respective setpoints were  $7.2 (\pm 0.2)$ ,  $11.6 (\pm 0.3)$ , and  $18.6 (\pm 0.5)$  V respectively, while the corresponding average current densities were  $0.86 (\pm 0.02)$ ,  $1.94 (\pm 0.08)$ , and  $4.08 (\pm 0.12)$  A/L.  $N = 800$  for each of these data. Note that the hardware consistently reported a lower measured current than the set point, leading to slightly lower current densities than the setpoint (also

accounting for the 10 mL (2%) decrease in culture volume after sampling at each time point). While the setpoint and their actual current densities differ slightly, they are referred to together as the setpoint values of 1 A/L, 2 A/L, and 4 A/L throughout the rest of this manuscript. The small spikes observed in the voltage traces correspond to the electrodes being shifted to allow cell build up to re-homogenize before sampling as described in the materials and methods section. Fig. 5A provides a visual representation of the effects of current density on flocculation. To confirm that membrane separated electroflocculation does protect the algal culture from bleaching a single test was run with carbon electrodes at 1 A/L treatment without a membrane. The unprotected culture was observed to bleach completely after 10 min of treatment.

Fig. 5A and C show that higher current densities achieve a 90% settling efficiency considerably faster than lower set points when settling for one hour (5 and 10 min for 4 and 2 A/L respectively compared to 30 min for 1 A/L). This corresponds to the rapid increases in pH observed in Fig. 6A, with culture reaching a pH of  $\sim 10$ , and subsequent OH<sup>-</sup> generation going to Mg(OH)<sub>2</sub> salt precipitation.<sup>27</sup> However, Fig. 5–7 show that the current density set point of 1 A/L has several critical advantages compared to higher setpoints. First, the linear volumetric energy requirement trends summarized in Fig. 5B show approximately two-fold and 4-fold higher slopes for 2 A/L and 4 A/L respectively. Even at 5 min and 10 min for the higher setpoints, the required energy is still well above the 1 A/L energy requirements at either 30 or 40 min of treatment. This is relevant as the 1 A/L setpoint power requirement for >90% settling efficiency is below the corresponding 2 A/L and 4 A/L values. This settling efficiency is shown in Fig. 5C, and the time required to reach above 90% settling efficiency for 4 A/L, 2 A/L and 1 A/L was measured to be 5, 10, and 30 min respectively.

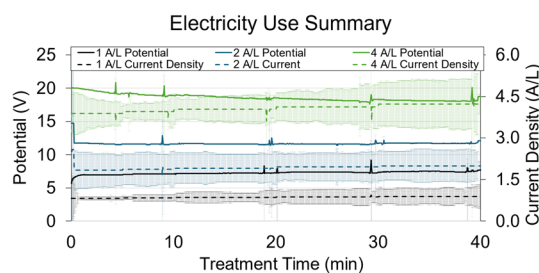


Fig. 4 A summary of the average current densities and voltages recorded during the set current treatments. A = amperage, V = voltage, L = liters. Values are the average of 3 tests, and the error bars represent standard deviations.

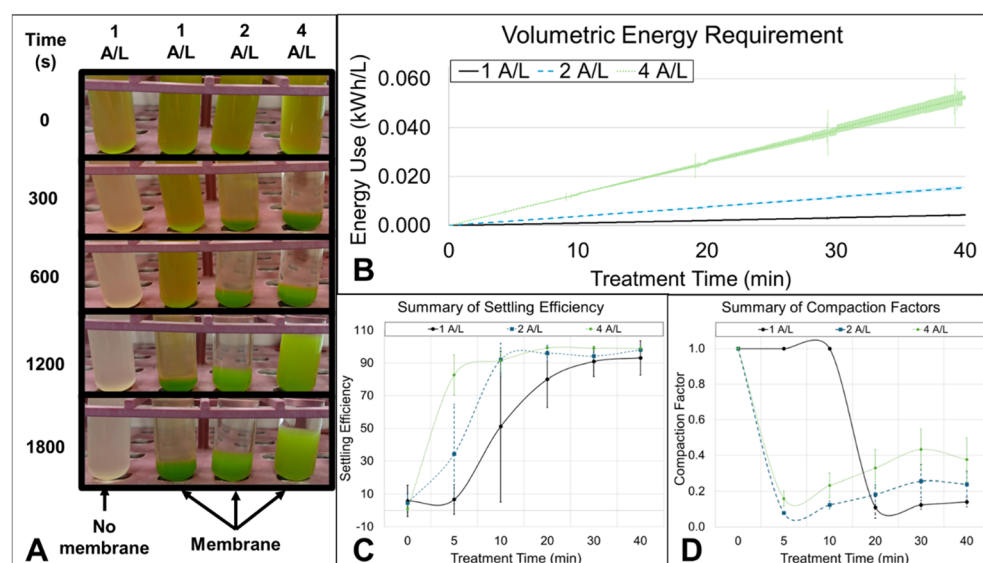


Fig. 5 (A) Representative photographs of the treated culture samples after settling one hour. Visually it can be seen that current density influences the speed of flocculation and compaction factor. (B) Shows the corresponding energy requirements on a volumetric basis. (C) and (D) show the measured values of settling efficiency and compaction factor across the time course, respectively.



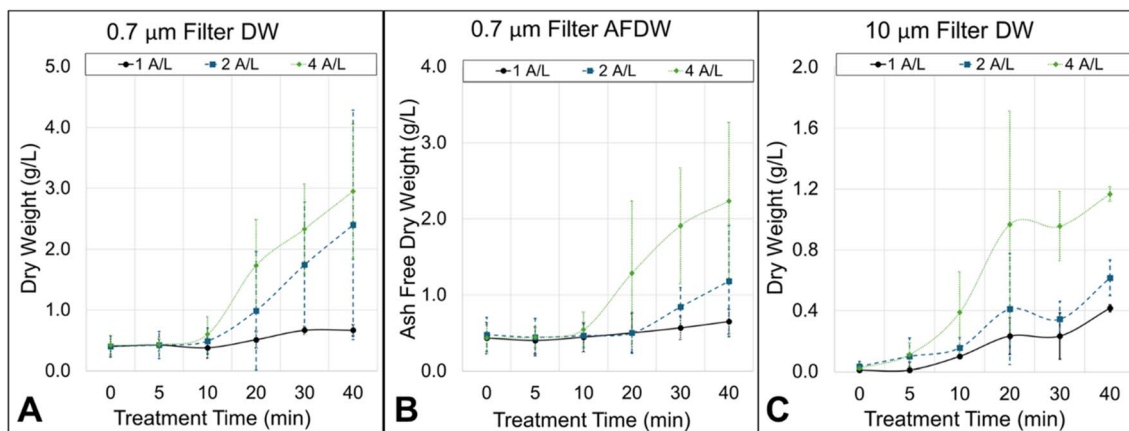


Fig. 6 A summary of the biomass measurements made at various current densities. 0.7  $\mu\text{m}$  filtration was used to measure the total DW, and AFDW, whereas 10  $\mu\text{m}$  filters were used to assess mass retention at a higher average pore size to demonstrate improved harvestability. (A) Dry weights and (B) AFDW measurements of samples filtered at 0.7  $\mu\text{m}$ . (C) Dry weights at 10  $\mu\text{m}$ . Values are the average of three tests and error bars represent standard deviation. Note that the y-axis scale varies in each panel.

Variability is high before settling efficiency plateaus at these time points. Compaction factors are shown in Fig. 5D. The 2 A/L and 4 A/L setpoints reach minimums of 0.08 ( $\pm 0.001$ ) and 0.16 ( $\pm 0.04$ ) at 5 min, followed by an increase to 0.2 and 0.4. The 1 A/L setpoint reached a compaction factor of 0.12 at 30 min. Based on these values, the average compaction layer AFDW was calculated to increase to 2.8, 5.6, and 3.8  $\text{g L}^{-1}$  at the respective setpoints of 4 A/L, 2 A/L and 1 A/L.

Additionally, Fig. 5D shows that at 2 A/L and 4 A/L the compaction factor increases after 10 min of treatment. This is due to an accumulation of salts that also impacts DW and AFDW measurements (Fig. 6A and B), indicating that there is a relatively narrow window of treatment at these setpoints time before the culture is “over-treated”. Mass increases above cellular biomass concentrations (time zero measurements) are due to the accumulation of inorganic salts alongside flocculated cells. This excludes carbonates for AFDW which volatilize during ashing. The results in Fig. 6 also indicate that some of the precipitate is adhering to the flocculated cells strongly enough to not be washed or volatilized during the filtration wash or ashing steps, respectively. The increase in DW across the treatment period at 2 A/L and 4 A/L and the corresponding increase in AFDW values show that salt accumulation can more than double the untreated biomass measurement. In contrast, DW and AFDW measurements for the 1 A/L setpoint show little to no increase across the treatment period. This result must be taken into consideration when interpreting the total mass retention at 10  $\mu\text{m}$  (Fig. 6C), as an increase in retention of samples treated at 1 A/L (up to about 65% of the total DW) is mostly biomass and not salt. Regardless of the current setpoint, there is a clear improvement in harvestability at 10  $\mu\text{m}$  after treatment, as by 40 min, mass retention at 10  $\mu\text{m}$  for 1 A/L, 2 A/L and 4 A/L reached 62.5, 25.7 and 39.5% of the corresponding 0.7  $\mu\text{m}$  DW value. No AFDW values could be obtained at 10  $\mu\text{m}$  as the filter material (polycarbonate) was combustible.

Also indicating better performance at 1 A/L are the corresponding temperature and pH profiles of the anode and cathode solutions presented in Fig. 7. As shown in Fig. 7A and B,

temperatures in both solutions remain slightly below room temperature at 1 A/L, but increases steadily during treatment at 2 A/L and 4 A/L. The final temperature at 4 A/L increases by 13  $^{\circ}\text{C}$ , whereas the 2 A/L tests show an increase of only  $\sim 3$   $^{\circ}\text{C}$ . The increase in cathode chamber pH is slower for the 1 A/L treatment. The observed increase in the cathode solution pH happens within 5 min at the two higher setpoints, but requires 20 min at 1 A/L. Within the anode chamber the plateau values are reached in all cases before 5 min.

An increase in temperature indicates reduced energy efficiency as current is converted to heat. Another source of heat could be excessive exothermic salt formation, as the 2 A/L and 4 A/L current setpoints reach a pH of 10 rapidly (<5 min), and hydroxide generated after that point went to salt formation. In either case, the temperature increase also leads to more evaporation from the system, also impacting the content of the gas products of the system. At 1 A/L the temperature remains constant around room temperature, showing that the lower current density setpoint is wasting less energy as heat. There is a small initial drop in temperature due to the action of the snorkel hood vacuum pulling air away from the system. This drop is less pronounced in the anode solution, likely due to the smaller surface area/volume ratio and overall volume of the anode chamber. It is possible that this artificial cooling also impacts the steady temperature increases at 2 A/L and 4 A/L, with both trends underestimating the actual temperature increase.

Taken together, these results are evidence that the 1 A/L setpoint is advantageous over the higher current densities, despite a longer time requirement to achieve flocculation. For this reason, additional tests were focused on using the 1 A/L setpoint.

### 3.2 Mechanism of protection from bleaching by the membrane

The evidence of culture protection from bleaching shown in Fig. 4–7 must be explained through seawater electrochemistry



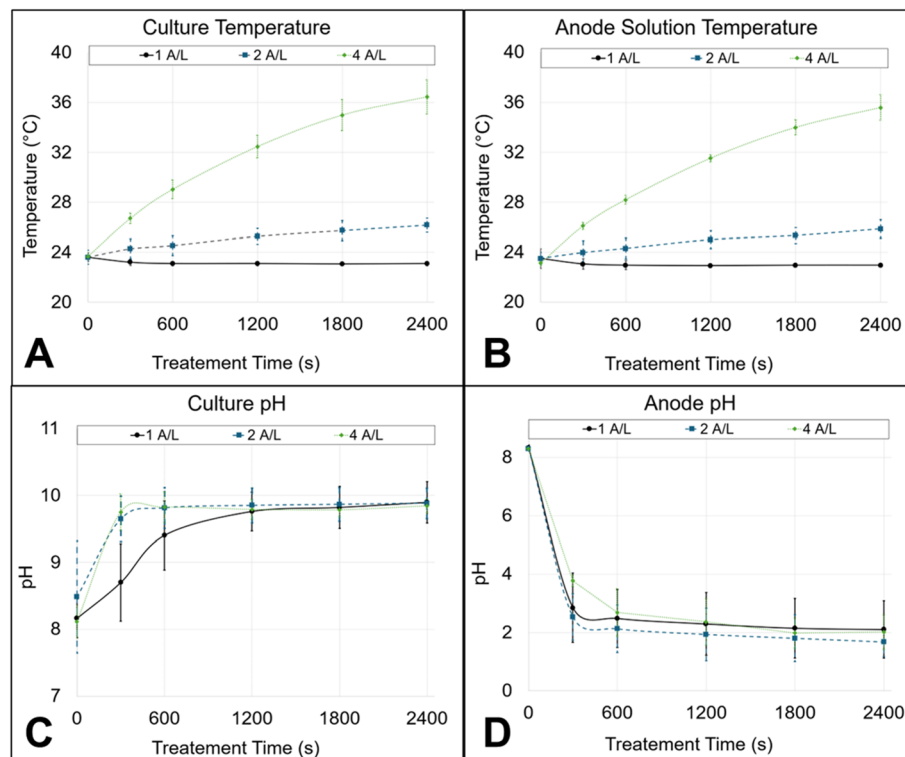
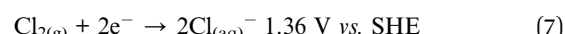
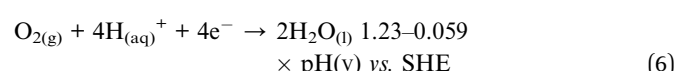
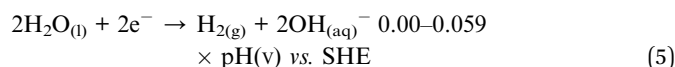


Fig. 7 Temperature changes in (A) the cathode (culture) solution and (B) the anode solution at various treatment setpoints. In both cases the 1 A/L samples remain stable around room temperature in contrast to semi-linear increases at 2 A/L and 4 A/L. (C) and (D) show the pH changes in the culture and anode solutions. In the culture, pH increases to 10, then plateaus. The anode solution begins to plateau at a pH of ~2 within 5 min.

and carbon speciation. The goal of contemporary seawater electrolysis work is producing H<sub>2</sub> by splitting H<sub>2</sub>O, and Cl<sub>2</sub> is an undesirable by-product.<sup>17</sup> On the other hand, wastewater electrolysis is used extensively for de-chlorination.<sup>28</sup> Beyond this, carbon partitioning and calcium carbonate precipitation have been thoroughly studied to understand their environmental and geological impact.<sup>29,30</sup> All three of these fields contribute important context for this work. Seawater in equilibrium with air is primarily speciated as bicarbonate, and that equilibrium pH is approximately 8.2, with variability due to the alkalinity of the medium. Moreover, the precipitation of calcium carbonate begins immediately as the pH rises and carbonate becomes the dominate carbon species at pH 12.<sup>31</sup> It also contains a large amount of dissolved chloride (up to 55% of the water ion composition).<sup>17</sup>

In a seawater electrolysis system, H<sub>2</sub> forms at the cathode along with both O<sub>2</sub> and Cl<sub>2</sub> at the anode. Eqn (5), written here in the anodic convention, shows the hydrogen evolution reaction (HER). Eqn (6) and (7) detail two of the possible anodic half reactions: the oxygen and chlorine evolution reactions (OER and CER). Included are the pH-dependent reduction potentials compared to a standard hydrogen electrode (SHE).<sup>32,33</sup>



In general, the OER and CER require higher overpotentials due to sluggish kinetics and mass transport compared to the HER.<sup>34</sup> As seen by comparing the potentials for OER and CER, O<sub>2</sub> formation should be favored over Cl<sub>2</sub> generation during electrolysis. However, OER requires larger overpotentials, making CER kinetically favorable. In addition, acidification of the anode compartment compared to the cathode compartment shifts the reaction potential of the anode to higher values, further favoring pH-independent CER. The alternate reactions by Cl<sup>-</sup> to form oxidative species are complicated by sensitivity to a variety of factors, including pH and the concentration of other ion species in the solution. However, the unadjusted redox potentials for these reactions are generally below 2 V,<sup>35</sup> so the formation of these products is inevitable with the high potentials required to achieve flocculation in this study.

Despite the presence of these oxidative species, Fig. 8 summarizes evidence that the algal cells remain viable after electrolysis treatment and neutralization with 350  $\mu\text{L}$  of 3 M hydrochloric acid. The acid was added dropwise to 100 mL of culture drawn off at the final timepoint (After the 20 min of mixing with no current shown in Fig. 9). The data corresponds to the 0.92 g L<sup>-1</sup> culture test reported in Fig. 10. Upon treatment the cell count decreased from 49.9 ( $\pm 1.3$ ) to 4.5 ( $\pm 0.1$ ) and after neutralization returned to 49.9 ( $\pm 0.7$ ). Fig. 8C shows that forward scatter – as a representation of cell size – increased by



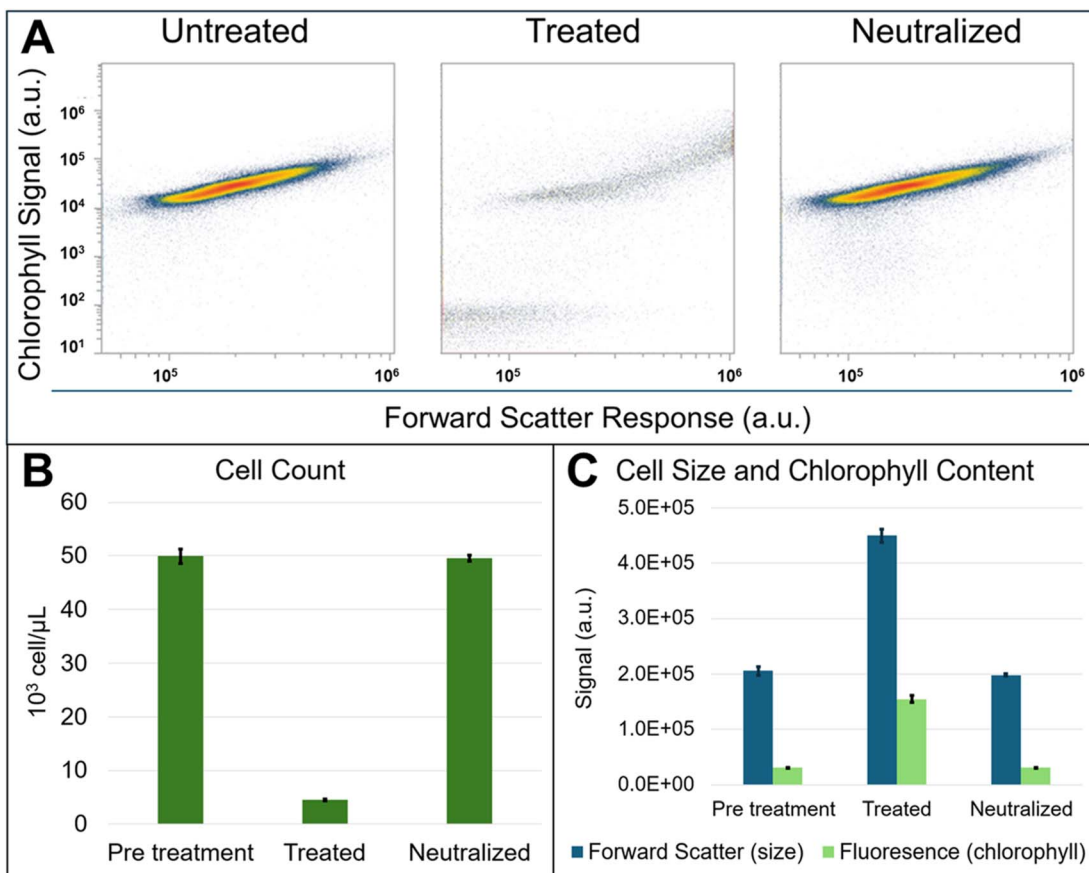


**Fig. 8** (A) Representative flow cytometry scatterplots show a shift between the untreated, treated, and neutralized culture. The x-axes report the height of the forward scatter peak, and the y-axis indicates the height of the chlorophyll signal peak. (B) Cell counts using flow cytometry before electroflocculation treatment, after treatment, and after neutralization with 3 M HCl. (C) The average size and chlorophyll fluorescence of the cells increases after treatment but reverts fully after neutralization.

2.2-fold, and the chlorophyll fluorescence of measured particles also increased by 5.0-fold. After neutralization, the original cell size and chlorophyll content were restored. The flow cytometer collection parameters (voltage, gain, *etc.*) were not changed between the treated and untreated measurements. The low standard deviation of the cell size and chlorophyll content of the treated samples is likely the result of the treated signal

increasing to the limit of the instrument detection range rather than a uniform size of flocculated cell clumps. The data presented in Fig. 8 both confirm the reversibility of the flocculation process by pH neutralization and provide evidence that the cells remain intact after neutralization. This was confirmed by microscopic observation (data not shown). While the retention of cell count, size, and chlorophyll content indicates little to no cell lysis during flocculation and neutralization, additional work is needed to determine if the cells remain viable for growth after this stage, and what effect this treatment has on the biomass composition.

A lack of culture bleaching (Fig. 5A and 8) shows that the membrane is protecting the culture from oxidative products generated at the anode. Solution pH was also used as an indicator of effective separation by the membrane between the acidic anode solution and basic culture, and as a clue about the potential mechanism of protection by the membrane. Fig. 9 shows the pH change of the membrane-separated cathode and anode solutions over time. Cathode solution pH increases to  $\sim$ pH 10 and then plateaus, while the anode solution pH drops to  $\sim$ 2.5. When the current is switched off at 40 min the pH difference between the two solutions remains. Values are the average of  $N = 9$  tests corresponding to the variable biomass tests presented in Fig. 10. Error bars represent standard deviation.

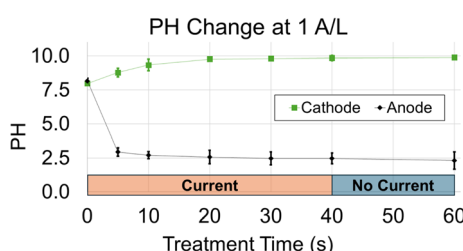


**Fig. 9** Change in pH of the cathode (culture) and anode solutions during treatment. The culture pH increases to  $\sim$ pH 10 and then plateaus, while the anode solution pH drops to  $\sim$ 2.5. When the current is switched off at 40 min the pH difference between the two solutions remains. Values are the average of  $N = 9$  tests corresponding to the variable biomass tests presented in Fig. 10. Error bars represent standard deviation.



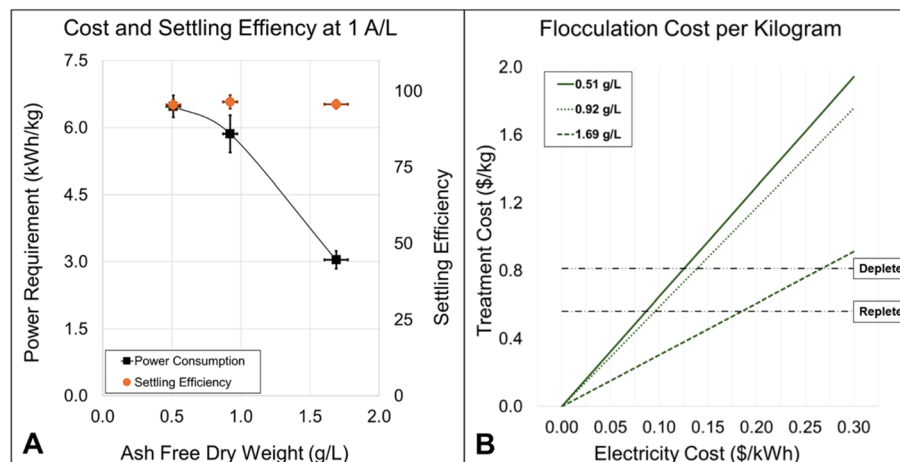


Fig. 10 A) Cost and efficiency of biomass treatment. Across three representative biomass densities ( $0.51, 0.92$ , and  $1.68\text{ g L}^{-1}$ ), the power requirement for treatment per unit biomass decreased whereas settling efficiency remained consistent at around 95%. (B) The cost of treatment per unit biomass over a range of electricity costs as calculated from the values shown in panel A. For comparison, the previously reported nutrient replete and nutrient deplete biomass values of *P. celeri* TG2 are shown as flat lines at  $0.56\text{ \$/kg}$  and  $0.81\text{ \$/kg}$  respectively.<sup>6</sup>

measured to test for an increase in anode pH or drop in cathode pH that could indicate diffusion across the membrane. However, anode solution and culture pH remained stable despite steady mixing. It is worth noting that the anode solution liquid height was 1.5 cm above the cathode solution during these tests (Fig. 2). This allowed greater potential for the anode solution to permeate to the cathode due to pressure, which further enforces the protective capability of the membrane in the system.

With no current, electro-osmotic flow across the membrane is zero, and the membrane material molecular weight cutoff (12–14 kDa) is far larger than the small ions or oxidative species that will diffuse across it following concentration gradients. Therefore, the observed lack of pH equilibration over 20 min indicates diffusion-limited transport through the membrane despite the thermodynamic driving force of the pH differential, likely diffusion is still occurring as current can run through the system, so charged species can cross the membrane, but the diffusion timescale is long (minutes to hours). A reduction in diffusion of  $\text{H}^+$  or  $\text{OH}^-$  across the membrane could be due to competitive ion diffusion of chloride (into the anode solution) and divalent metals (into the cathode solution) as these ions are removed during electrolysis through outgas and precipitation, respectively. Membrane polarization can also reduce the diffusion of ions across the membrane.<sup>36,37</sup> However, polarization also increases resistance, so the membrane would need to have been polarized early in the process as current and voltage do not increase noticeably across the treatment period (Fig. 4). Finally, the relatively small volume of the anode solution (20% of the culture) and mixing in the cathode helps quickly dilute any products moving from the anode solution to the culture. It is possible that several of these effects are contributing to the protective capability of the membrane simultaneously. One effect that can be ruled out is membrane fouling due to organic product adhesion as the differential pH result was also observed in tests using seawater without microalgae (data not shown).

With respect to the diffusion of oxidative species from the anode, another effect is likely contributing to limit culture damage. Previous literature shows that as a solution pH decreases to below 4,  $\text{Cl}_2$  is formed in competition with hypochlorous acid, and becomes the dominant product at pH 2 or below.<sup>35,38,39</sup> As the anode headspace was continuously removed by the action of the vacuum snorkel,  $\text{Cl}_2$  outgassing from the anode solution left the system. This resulted in less opportunity for cross reaction to form  $\text{ClO}_x$  products, and additional  $\text{Cl}_2$  formation as the system shifts toward equilibrium. However, measurements of  $\text{Cl}_2$  gas production or oxidative species formation were not performed in this study, so additional experiments are needed to provide direct evidence supporting this effect and the overall mechanism of protection within this system.

### 3.3 Integration of electroflocculation into a microalgal biomass pipeline

While testing across a range of biomass concentrations at 1 A/L (shown in Fig. 10) the settling efficiency remained at an average of 95.9%. Conversely, estimated biomass flocculation cost decreased in a near linear trend. The corresponding average power consumption and standard deviation at 0.51, 0.92 and  $1.68\text{ g L}^{-1}$  densities were  $6.5\text{ kWh kg} (\pm 0.2)$ ,  $5.9\text{ kWh kg} (\pm 0.4)$ , and  $3.0\text{ kWh kg} (\pm 0.2)$ . The corresponding cost of treatment overcomes the intrinsic value of nutrient-replete *P. celeri* TG2 biomass at electricity prices of 0.9, 0.10, and  $0.18\text{ \$/kWh}$ . Both settling efficiency and power requirement are based on 1 h of settling time with 30 min of treatment time.

The range of biomass densities tested in Fig. 10 was chosen to be relevant to pond cultures.<sup>40–42</sup> Two conclusions arise from the results shown in Fig. 10A: first, a settling efficiency of >90% is achieved by 30 min regardless of concentration, and second, the power required for treating the biomass decreases in a near-linear trend, indicating that power requirement remains relatively constant across the biomass range tested. Based on the



costs presented in Fig. 10B, the cost of treatment is less for thicker cultures. A major drawback indicated by these results is that the flocculation cost can exceed the intrinsic biomass value of *P. celeri* TG2 as the price of electricity increases. The electricity cost will have a major impact on the viability of this technology in any harvesting scenario, so for this technique to be a useful addition to the harvesting pipeline for pond biomass, the power requirement of the system must be improved.

This may be accomplished by reducing the resistance in the system through variables such as reactor geometry, electrode material, membrane composition, and anode solution makeup. Even at the 1 A/L setpoint, the voltage required for hydrolysis remained at 7.2 V (Fig. 4), which is well above the potentials required for the OER and CER reactions (with the HER requiring even less potential). This indicates ohmic resistance throughout the cell is being increased.<sup>37</sup> There are several sources of added resistance within this system design (Fig. 2) that also represent possible ways to reduce treatment cost. First, the 1 A/L current setpoint is still likely not the optimal current density to achieve flocculation without loss to heat, and lower setpoints can be tested with the trade-off of increasing required treatment time. Second, the membrane and electrode material can be altered to reduce resistance, such as an ion exchange membrane. Similarly, the carbon cathode can be replaced with a more catalytically efficient material such as copper, and the anode with an inert alternative such as titanium. However, replacing the electrodes or membrane with more expensive material will increase the initial cost of building the system. Third, the system geometry can be altered to reduce distance between the electrodes, and/or increase the surface area to volume ratio of the electrodes. Fourth, the anode solution can be altered to an even more conductive composition, such as saturated sodium chloride. Together these options represent possible avenues of exploration for future studies.

In the context of current literature, this work is a complement to a publication by Zhu *et al.* who reported on flocculation data for *Picochlorum oklahomensis*. They measured a flocculation efficiency better than 95% after 5–20 minutes of treatment with aluminum electrodes operated in a range of 0.8–3.2 A/L and settling times ranging from 0.5–12 h.<sup>25</sup> A direct cost comparison is not possible as the study did not report voltage or power requirement, however the sacrificial aluminum electrodes are more efficient than those in this study particularly in terms of the required treatment time. Another relevant comparison for the results of this study is the salt bridge electroflocculation technique recently published by Hou *et al.*<sup>19</sup> The electrical energy consumptions are similar, with a reported energy requirement of 3.61 kWh kg for 30 min of treatment at a current density of 1.2 A/L and a biomass concentration of 1.4 g L<sup>-1</sup> and a recovery (settling) efficiency of 96%. However, they also report that reducing the treatment current to 0.85 A/L for 45 min reduced the energy consumption to 1.5 kWh kg, with a corresponding recovery efficiency of 90%. Based on this, lower current setpoints than those tested in this study should be explored to find the optimal energy requirement for flocculating *P. celeri*.

The results presented here should also be considered within context of treating a large algal culture within a reasonable period. Optimizing parameters such as treatment time, settling time, and current setpoint is also a strategy to reduce power consumption. Current density should be selected to balance required treatment time and energy efficiency, and a setpoint at or below 1 A/L was shown to accomplish this. Also, while this study focuses on a relatively short settling period (1 hour), a longer period will increase settling efficiency and compaction factor. Depending on the requirements of a larger system, this parameter can be adjusted to balance time and the effectiveness of settling. Finally, mixing is a critical consideration in these experiments. A larger scale harvesting system will mix in a significantly different manner depending on the system configuration, and the change in flocculation behavior if salt precipitates do not form uniformly throughout the system will need to be understood and accounted for.

The membrane material used for this treatment should also be carefully considered in future work. Regenerated cellulose was used in this study as it is relatively cheap, easily available, and physically flexible enough to be integrated into the anode chamber used (Fig. 3). However, regenerated cellulose is not hydrolytically stable, especially at high or low pH,<sup>43</sup> so the next step in this work is to utilize pH stable membrane materials such as polyethersulfone. Although this membrane is less hydrophilic than regenerated cellulose,<sup>44</sup> the relatively large molecular weight cutoffs available (>10 kDa, as demonstrated in this work) still allows for diffusion and electroosmosis. Integrating a hydrolytically stable anion exchange membrane may be even more useful, as it would improve conductivity across the membrane, and selectively block positively charged compounds from diffusing to cathode solution from the anode solution.<sup>45</sup>

The inspiration for this study came from the chlor-alkali process. A method for generating industrial quantities of Cl<sub>2</sub> and NaOH that has been well established for more than a century. In membrane-based operation, the chlor-alkali process utilizes ion exchange membranes,<sup>46</sup> and these may provide better efficiency than the regenerated cellulose material used in this study. Also, the chlor-alkali process utilizes a prepared brine of approximately 25% w/v NaCl with no impurities such as divalent cations, trace metals, and sulfur-based ions to maximize the efficiency of current transfer and prevent precipitates that can take up active sites on the cathode. As applied in this case, a clean brine solution is not practical for the cathode solution but could be used in the anode. Alongside this, the seawater used to cultivate microalgae may eventually be depleted of calcium and magnesium if the medium is recycled. However, the removal of these divalent metals opens the possibility of high bicarbonate cultivation in the recycled saline medium, as the carbonate will not be lost as a precipitate.<sup>47</sup> This is one potential use of the clarified growth medium, which is already at pH 10. Other methods and recycling should be considered over neutralizing the medium as it would likely be cost-prohibitive. The handling of the acidified anode solution is another hurdle in this process. The total volume can be much less than that used for culturing, so recombination with the basic treated solution may be the simplest approach to



neutralization. Another important consideration is that  $\text{Cl}_2$  and  $\text{H}_2$  will need to be safely removed and repurposed from the system. One partial solution is a sealed continuous flow anode solution which can capture the  $\text{Cl}_2$  and prevent outgassing.

Looking beyond flocculation to biomass refinement, a potential advantage of this technique is also apparent. Because of the addition of  $\text{OH}^-$  and  $\text{CO}_3^{2-}$  to biomass during this process, it is possible that treatment will integrate favorably with hydrothermal liquefaction (HTL) to produce biocrude. HTL is done at elevated temperature and pressure, and can be improved by the addition of a homogenous alkaline catalyst such as KOH or  $\text{Na}_2\text{CO}_3$ .<sup>48</sup> However, it was previously stated that this catalyst must be recovered to make the addition economically viable. By the precipitation of catalyst during non-sacrificial electrode flocculation, it is possible that this technoeconomic hurdle could be mitigated.<sup>49</sup>

## 4. Conclusions

This study demonstrates the feasibility of membrane-separated non-sacrificial electrode flocculation as a method for harvesting *P. celeri* TG2 grown in seawater. Through membrane separation, the harmful effects of  $\text{Cl}_2$  gas generation were mitigated while achieving effective flocculation through pH-mediated salt precipitation. The results indicate that this method protects the algal culture and maintains a settling efficiency of  $\geq 95\%$  across a biomass concentration range of  $0.51\text{--}1.68 \text{ g L}^{-1}$ . A current density setpoint of  $1 \text{ A/L}$  was found to provide a reasonable balance of energy efficiency and required treatment time. However, this is not an optimized setpoint, and the total cost of treatment is sensitive to the price of electricity so care must be taken that the flocculation cost is well below the biomass value of the algae.

Membrane integration represents new possibilities for successfully flocculating microalgae, particularly small cells that may require pre-flocculation to improve settling and/or filterability. The power consumption data reported here are lower than literature reports for inert electrode flocculation in freshwater<sup>15,21,22</sup> and similar to results reported in saltwater.<sup>19</sup> A remaining challenge of using non-sacrificial electrodes in seawater is the production of  $\text{Cl}_2$  gas during the process. This work has opened a variety of experimental avenues that can be pursued to better understand how a system utilizing non-sacrificial electrodes can be constructed to minimize electricity input, maximize flocculation, and effectively reuse the products of electrolysis.

## Author contributions

Galen Dennis: conceptualization, funding acquisition, methodology, investigation, data curation, formal analysis, visualization, writing – original draft, writing – review & editing. Devin A.J. Karns: methodology, investigation, resources, writing – review & editing. Matthew C. Posewitz: supervision, writing – review & editing.

## Conflicts of interest

There are no conflicts to declare.

## Data availability

The data supporting this article have been included as part of the supplementary information (SI). Supplementary information: data included are the all of the electricity usages and physiological measurements used to produce the figures presented in the manuscript. See DOI: <https://doi.org/10.1039/d5ra07757e>.

## Acknowledgements

This work was partially funded by the 2023–2025 AlgaePrize finalist award provided by the U.S. Department of Energy through The Algae Foundation.

## References

- 1 T. L. Chacón-Lee and G. E. González-Mariño, Microalgae for “Healthy” Foods—Possibilities and Challenges, *Compr. Rev. Food Sci. Food Saf.*, 2010, **9**(6), 655–675.
- 2 J. C. Weissman, M. Likhogrud, D. C. Thomas, W. Fang, D. A. J. Karns, J. W. Chung, *et al.*, High-light selection produces a fast-growing *Picochlorum celeri*, *Algal Res.*, 2018, **36**, 17–28.
- 3 A. Krishnan, M. Likhogrud, M. Cano, S. Edmundson, J. B. Melanson, M. Huesemann, *et al.*, *Picochlorum celeri* as a model system for robust outdoor algal growth in seawater, *Sci. Rep.*, 2021, **11**(1), 11649.
- 4 B. Klein and R. Davis, Algal Biomass Production via Open Pond Algae Farm Cultivation: 2021 State of Technology and Future Research, *Renewable Energy*, 2022, **32**, 2–19.
- 5 Y. Zarmi, J. M. Gordon, A. Mahulkar, A. R. Khopkar, S. D. Patil, A. Banerjee, *et al.*, Enhanced Algal Photosynthetic Photon Efficiency by Pulsed Light, *iScience*, 2020, **23**(5), 101115.
- 6 B. C. Klein, R. E. Davis and L. M. L. Laurens, Quantifying the intrinsic value of algal biomass based on a multi-product biorefining strategy, *Algal Res.*, 2023, **72**, 103094.
- 7 R. Davis, A. Aden and P. T. Pienkos, Techno-economic analysis of autotrophic microalgae for fuel production, *Appl. Energy*, 2011, **88**(10), 3524–3531.
- 8 S. R. Ravichandran, C. D. Venkatachalam, M. Sengottian, S. Sekar, S. Kandasamy, K. P. Ramasamy Subramanian, *et al.*, A review on hydrothermal liquefaction of algal biomass on process parameters, purification and applications, *Fuel*, 2022, **313**, 122679.
- 9 A. I. Barros, A. L. Gonçalves, M. Simões and J. C. M. Pires, Harvesting techniques applied to microalgae: A review, *Renewable Sustainable Energy Rev.*, 2015, **41**, 1489–1500.
- 10 J. P. F. Koren and U. Syversen, State-of-the-art electroflocculation, *Filtr.*, 1995, **32**(2), 153–156.
- 11 S. Visigalli, M. G. Barberis, A. Turolla, R. Canziani, M. Berden Zrimec, R. Reinhardt, *et al.*, Electrocoagulation–



flotation (ECF) for microalgae harvesting – A review, *Sep. Purif. Technol.*, 2021, **15**(271), 118684.

12 T. Chatsungnoen, Y. Chisti, Chapter 11 - Flocculation and electroflocculation for algal biomass recovery. In: *Biofuels from Algae*, ed. Pandey A., Chang J. S., Soccol C. R., Lee D. J. and Chisti Y., 2nd edn, Elsevier; 2019. p. 257–286, <https://www.sciencedirect.com/science/article/pii/B9780444641922000111>.

13 N. Uduman, Y. Qi, M. K. Danquah, G. M. Forde and A. Hoadley, Dewatering of microalgal cultures: A major bottleneck to algae-based fuels, *J. Renewable Sustainable Energy*, 2010, **2**(1), 012701.

14 L. Semerjian and G. Ayoub, High-pH-Magnesium Coagulation–Flocculation in Wastewater Treatment, *Adv. Energy Environ. Res.*, 2003, **7**, 389–403.

15 R. Misra, A. Guldhe, P. Singh, I. Rawat, T. A. Stenström and F. Bux, Evaluation of operating conditions for sustainable harvesting of microalgal biomass applying electrochemical method using non sacrificial electrodes, *Bioresour. Technol.*, 2015, **176**, 1–7.

16 D. Ghernaout, M. W. Naceur and B. Ghernaout, A review of electrocoagulation as a promising coagulation process for improved organic and inorganic matters removal by electrophoresis and electroflootation, *Desalin. Water Treat.*, 2011, **28**(1), 287–320.

17 J. Chang and Y. Yang, Advancements in Seawater Electrolysis: Progressing from Fundamental Research to Applied Electrolyzer Application, *Renewables*, 2023, **1**(4), 415–454.

18 S. L. Pahl, A. K. Lee, T. Kalaitzidis, P. J. Ashman, S. Sathe and D. M. Lewis. Harvesting, Thickening and Dewatering Microalgae Biomass, In: *Algae for Biofuels and Energy*, ed. Borowitzka M. A. and Moheimani N. R., Springer Netherlands, Dordrecht, 2013. p. 165–185, DOI: [10.1007/978-94-007-5479-9\\_10](https://doi.org/10.1007/978-94-007-5479-9_10).

19 Y. Hou, C. Liu, Z. Liu, T. Han, N. Hao, Z. Guo, *et al.*, A Novel Salt-Bridge Electroflocculation Technology for Harvesting Microalgae, *Front. Bioeng. Biotechnol.*, 2022, **10**, DOI: [10.3389/fbioe.2022.902524](https://doi.org/10.3389/fbioe.2022.902524).

20 A. L. G. Teixeira, *Evolution of Electroflocculation for Harvesting Dunaliella Salina Using Non Sacrificial Electrodes*, University of Porto, 2016, <https://hdl.handle.net/10216/89110>.

21 A. Guldhe, R. Misra, P. Singh, I. Rawat and F. Bux, An innovative electrochemical process to alleviate the challenges for harvesting of small size microalgae by using non-sacrificial carbon electrodes, *Algal Res.*, 2016, **19**, 292–298.

22 W. Li, Y. Zhang, Y. Hu, S. Luo, X. Wu, Y. Liu, *et al.*, Harvesting Chlorella vulgaris by electro-flootation with stainless steel cathode and non-sacrificial anode, *Bioresour. Technol.*, 2022, **363**, 127961.

23 A. Krishnan, M. Cano, T. A. Burch, J. C. Weissman and M. C. Posewitz, Genome editing using Cas9-RNA ribonucleoprotein complexes in the high-productivity marine alga *Picochlorum celeri*, *Algal Res.*, 2020, **49**, 101944.

24 G. Dennis and M. C. Posewitz, Advances in light system engineering across the phototrophic spectrum, *Front. Plant Sci.*, 2024, **15**, DOI: [10.3389/fpls.2024.1332456](https://doi.org/10.3389/fpls.2024.1332456).

25 Y. Zhu, N. T. Dunford and C. Goad, Effect of Processing Parameters on Flocculation of *Picochlorum oklahomensis*, *J. Am. Oil Chem. Soc.*, 2014, **91**(2), 317–324.

26 A. J. LaPanse, A. Krishnan, G. Dennis, D. A. J. Karns, L. R. Dahlin, S. Van Wychen, *et al.*, Proximate biomass characterization of the high productivity marine microalga *Picochlorum celeri* TG2, *Plant Physiol. Biochem.*, 2024, **207**, 108364.

27 Y. Sano, Y. Hao and F. Kuwahara, Development of an electrolysis based system to continuously recover magnesium from seawater, *Helijon*, 2018, **4**(11), e00923.

28 A. Ciblak, X. Mao, I. Padilla, D. Vesper, I. Alshawabkeh and A. N. Alshawabkeh, Electrode effects on temporal changes in electrolyte pH and redox potential for water treatment, *J. Environ. Sci. Health, Part A*, 2012, **47**(5), 718–726.

29 M. Rygel, Q. Page. Sedimentary Geology: Rocks, Environments and Stratigraphy [Internet]. 6.2.1 Carbonate Precipitation: SUNY Potsdam; 2025 <https://geo.libretexts.org/@go/page/20409>.

30 L. Irving, The Precipitation of Calcium and Magnesium from Sea Water, *J. Mar. Biol. Assoc. U. K.*, 1926, **14**(2), 441–446.

31 M. H. Ghobadi, M. Firuzi and E. Asghari-Kaljahi, Relationships between geological formations and groundwater chemistry and their effects on the concrete lining of tunnels (case study: Tabriz metro line 2), *Environ. Earth Sci.*, 2016, **75**(12), 987.

32 A. J. Bard and L. R. Faulkner, Chapter 2 Potentials and Thermodynamics of Cells. In: *Electrochemical Methods Fundamentals and Applications*, 2nd edn, John Wiley & Sons, INC., 2001, p. 44–86.

33 S. G. Bratsch, Standard Electrode Potentials and Temperature Coefficients in Water at 298.15 K, *J. Phys. Chem. Ref. Data*, 1989, **18**(1–21), 1–16.

34 F. Zhang, J. Zhou, X. Chen, S. Zhao, Y. Zhao, Y. Tang, *et al.*, The Recent Progresses of Electrodes and Electrolysers for Seawater Electrolysis, *Nanomaterials*, 2024, **14**(3), 1–26.

35 J. J. Kaczur, Oxidation chemistry of chloric acid in NOx/SOx and air toxic metal removal from gas streams, *Environ. Prog.*, 1996, **15**(4), 245–254.

36 S. K. A. Al-Amshawee and M. Y. B. M. Yunus, Electrodialysis membrane with concentration polarization – A review, *Chem. Eng. Res. Des.*, 2024, **201**, 645–678.

37 T. Binninger, A. Heinritz and R. Mohamed, Ideal gas reference for association/dissociation reactions: Concentration bias and kinetic reference voltage/potentials in electrolysis, *J. Chem. Phys.*, 2023, **158**(12), 124129.

38 D. Gombas, Y. Luo, J. Brennan, G. Shergill, R. Petran, R. Walsh, *et al.*, Guidelines To Validate Control of Cross-Contamination during Washing of Fresh-Cut Leafy Vegetables, *J. Food Prot.*, 2017, **80**(2), 312–330.

39 M. Deborde and U. von Gunten, Reactions of chlorine with inorganic and organic compounds during water treatment—Kinetics and mechanisms: A critical review, *Water Res.*, 2008, **42**(1), 13–51.



40 L. Novoveská, S. L. Nielsen, O. T. Eroldoğan, B. Z. Haznedaroglu, B. Rinkevich, S. Fazi, *et al.*, Overview and Challenges of Large-Scale Cultivation of Photosynthetic Microalgae and Cyanobacteria, *Mar. Drugs*, 2023, **21**(8), 445.

41 C. Inostroza, J. Dávila, S. Román, J. M. Fernández-Sevilla and F. G. Acién, Use of airfoils for enhancement of photosynthesis rate of microalgae in raceways, *J. Appl. Phycol.*, 2023, **35**(6), 2571–2581.

42 Y. Chisti, Biodiesel from microalgae, *Biotechnol. Adv.*, 2007, **25**(3), 294–306.

43 C. K. Falkenreck, J. C. Zarges and H. P. Heim, Degradation pathways and chemical stability of regenerated cellulose fiber-reinforced bio-polyamide 5.10 composites under acidic and alkaline conditions, *Sci. Rep.*, 2025, **15**(1), 35242.

44 M. Gryta and P. Woźniak, The Resistance of Polyethersulfone Membranes on the Alkaline Cleaning Solutions, *Membranes*, 2024, **14**(2), 27.

45 Strathmann H., ed. Chapter 3 - Preparation and Characterization of Ion-Exchange Membranes, In: *Membrane Science and Technology*, Elsevier, 2004, pp. 89–146, <https://www.sciencedirect.com/science/article/pii/S0927519304800342>.

46 E. Beaver, P. Pujado, D. Hertz, J. Hacsaylo, H. Burney, R. Alvarado and *et al.* *Energy and Environmental Profile of the U.S. Chemical Industry*, Columbia, Maryland, U.S. Department of Energy Office of Industrial Technologies, 2000, p. 175–200, [https://www1.eere.energy.gov/manufacturing/resources/chemicals/pdfs/profile\\_chap1.pdf](https://www1.eere.energy.gov/manufacturing/resources/chemicals/pdfs/profile_chap1.pdf).

47 X. Du, C. Zhu and Z. Chi, Optimizing calcium and magnesium in seawater medium with high bicarbonate concentration for efficient growth and self-flocculation harvesting of Chlorella sp, *Bioresour. Technol.*, 2025, **430**, 132569.

48 D. López Barreiro, W. Prins, F. Ronsse and W. Brilman, Hydrothermal liquefaction (HTL) of microalgae for biofuel production: State of the art review and future prospects, *20th Eur Biomass Conf*, 2013, **53**, 113–127.

49 A. A. Peterson, F. Vogel, R. P. Lachance, M. Fröling, Jr Antal, J. Michael and J. W. Tester, Thermochemical biofuel production in hydrothermal media: A review of sub- and supercritical water technologies, *Energy Environ. Sci.*, 2008, **1**(1), 32–65.

